

Supporting Information

A multifunctional nanoplatform based on mesoporous silica nanoparticles for imaging-guided chemo/photodynamic synergetic therapy

Yadan Liu,^{a,b} Xiaolin Liu,^a Yue Xiao,^{a,b} Fangman Chen,^{a,b} Fangnan Xiao^{a*}

a. State Key Laboratory of Structural Chemistry, Fujian Institute of Research on the Structure of Matter, Chinese Academy of Sciences, Fuzhou, Fujian 350002, China

b. College of Life Sciences, Fujian Agriculture and Forestry University, Fuzhou, Fujian 350002, China.

* To whom correspondence should be addressed.

E-mail: fnxiao@fjirsm.ac.cn

Tel.: +86-591-63173176

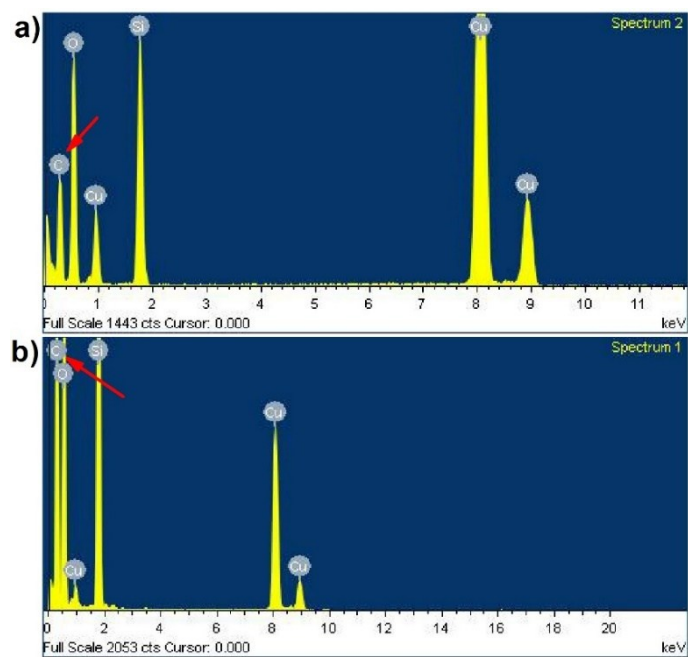


Figure S1. Energy-dispersive X-ray spectroscopy (EDX) pattern of a) mesoporous silica nanoparticles (MSNs) and b) MSN@C-dots nanoparticles. The EDX pattern revealed the presence of C, and Si elements in the MSN and MSN@C-dots nanoparticles. It should be noted that, the content of carbon element in MSN@C-dots was significantly higher than that of the MSNs.

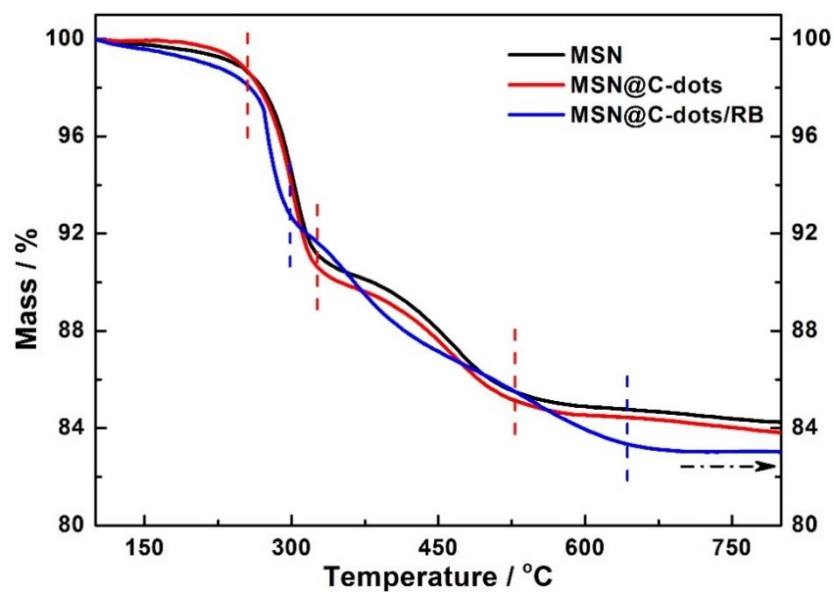


Figure S2. Thermogravimetric analyses (TGA) curves of MSNs, MSN@C-dots and MSN@C-dots/RB nanoparticles under N₂ atmosphere in the temperature range of 35-800 °C at a rate of 10 °C min⁻¹. Different decomposition temperatures and weight losses were observed, due to different composition of nanoparticles, which indicate the successful embedding of C-dots in MSNs as well as RB in MSN@C-dots/RB nanoparticles.

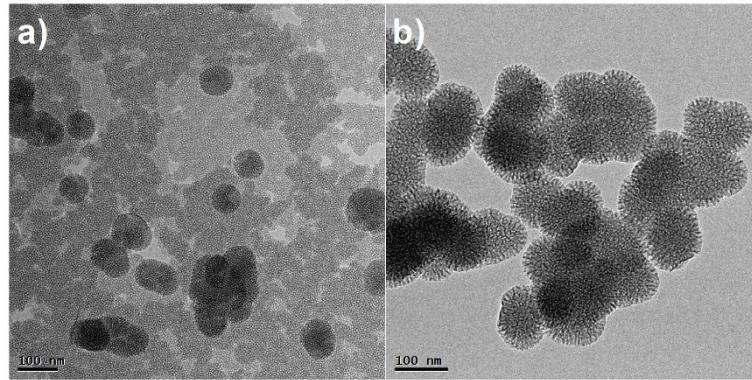


Figure S3. a) Transmission electron microscopy (TEM) image of MSNs doping with high concentration C-dots dopant (1.5 mg/mL). b) TEM image of MSN@C-dots doping with high concentration RB molecules (3 mM/mL). As shown in these TEM images, the morphologies of MSNs were seriously affected by higher doping concentration of C-dots or RB molecules.

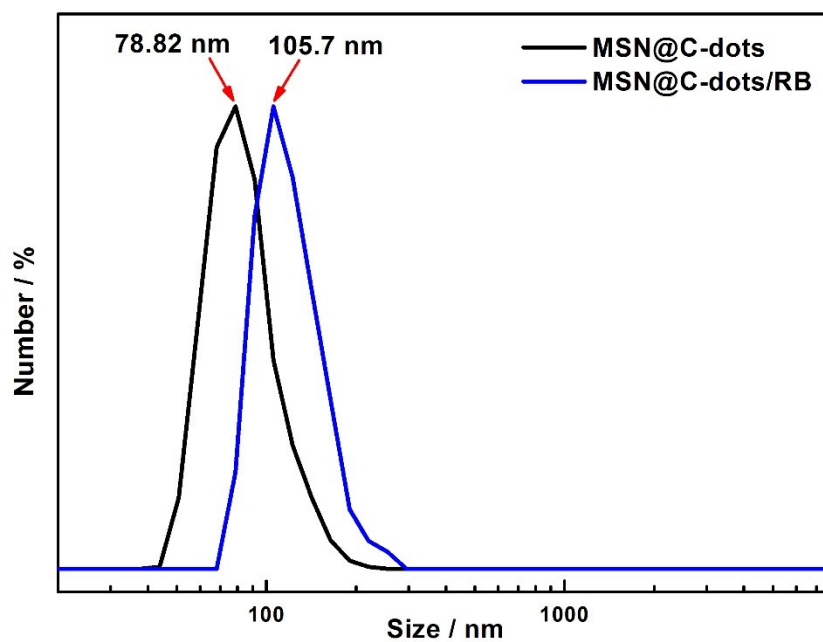


Figure S4. Hydrodynamic diameter distribution of the MSN@C-dots and MSN@C-dots/RB nanoparticles. The hydrodynamic diameter of the MSN@C-dots nanoparticles (78.82 nm) is in agreement with their TEM images. In comparison with MSN@C-dots nanoparticles, the hydrodynamic diameter of MSN@C-dots/RB nanoparticles increased from 78.8 nm to 105.7 nm, indicating that the mesoporous silica shell was successfully epitaxially grown on MSN@C-dots nanoparticles.

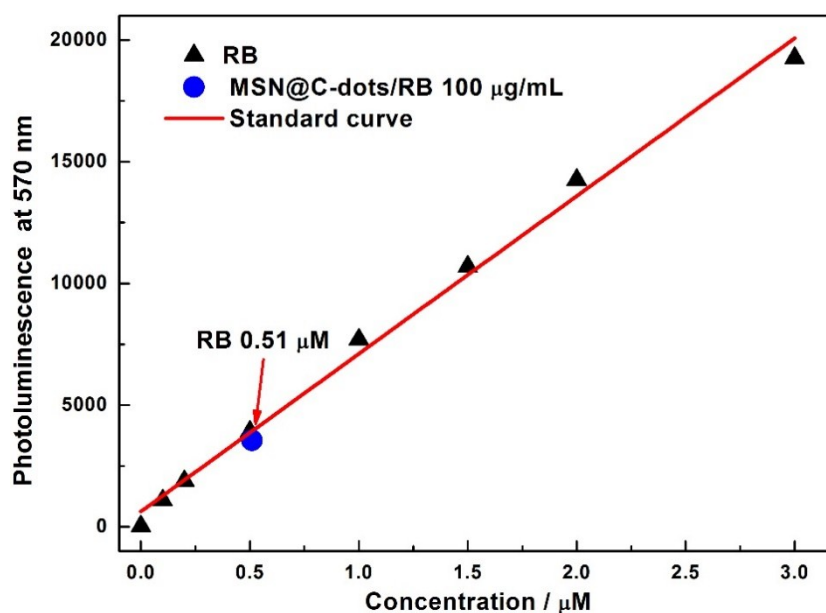


Figure S5. Quantitative analysis of Rose Bengal (RB) embedded in the MSN@C-dots/RB nanoparticles. The amount of RB was determined by measuring the Photoluminescence (PL) intensity of RB at 570 nm. Loading capacity of RB was calculated as follows: loading capacity (%) = (weight amount of RB in MSN@C-dots/RB nanoparticles) / (weight amount of MSN@C-dots/RB nanoparticles) \times 100 %. From the PL intensity of MSN@C-dots/RB nanoparticles, the content of RB in the MSN@C-dots/RB nanoparticles was quantified to be 0.52 % (w/w).

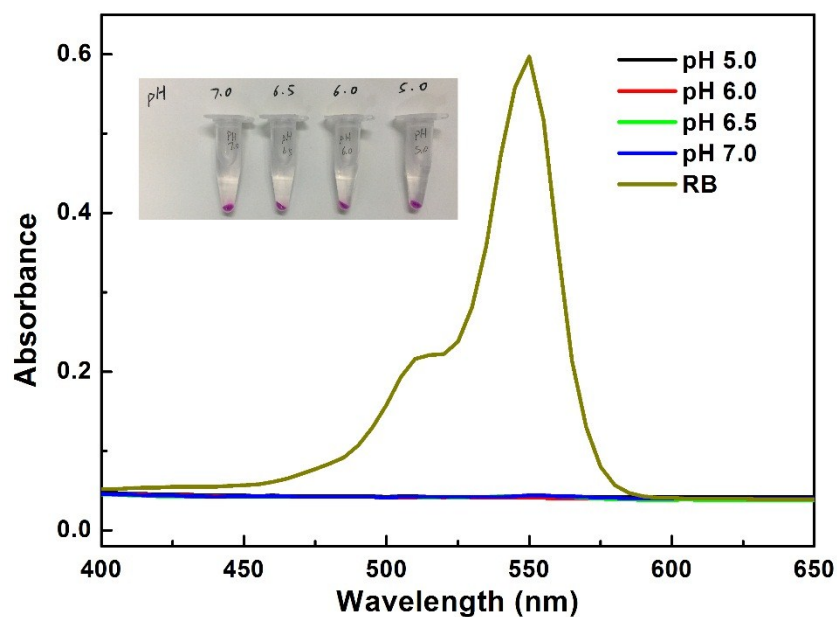


Figure S6. Absorption spectra of pure RB and the centrifugated supernatant of MSN@C-dots/RB nanoparticles after soaking for 72 hours in PBS buffer with different pH ranging from 5.0 to 7.0. As compared to that of pure RB, the absorbance of the photosensitizers in the supernatant of MSN@C-dots/RB nanoparticles solution can be neglected, indicating that a negligible low content of RB was released from MSN@C-dots/RB nanoparticles even for 72 hours soaked in PBS buffer. The inset shows the photographs of MSN@C-dots/RB nanoparticles soaked in PBS buffer with different pH. These results verify the high stability of the MSN@C-dots/RB nanoparticles.

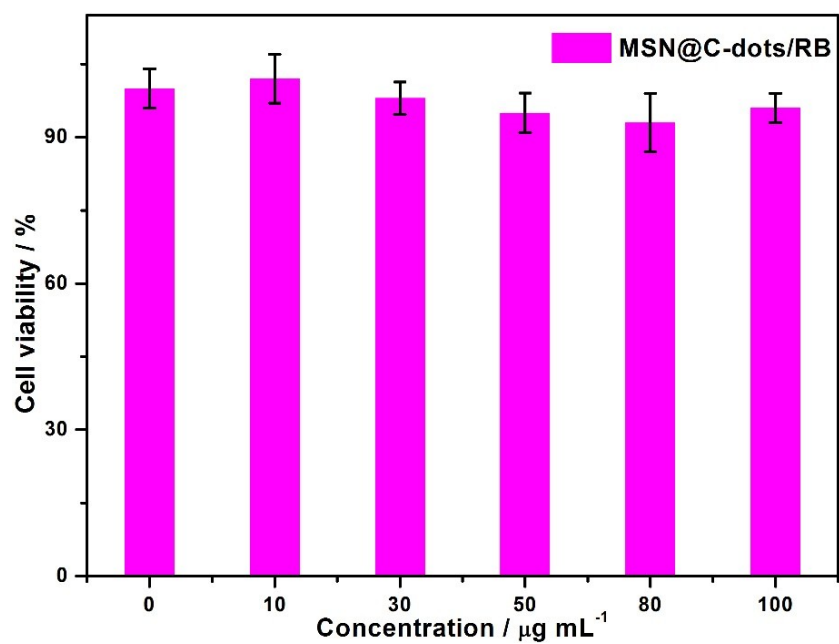


Figure S7. *In vitro* cytotoxicity of MSN@C-dots/RB nanoparticles against human embryo lung fibroblasts (HELF) cells after incubation for 24 h by using a MTT assay. The cell viability was determined to be higher than 90 % even at a concentration as high as 100 $\mu\text{g/mL}$ for the MSN@C-dots/RB nanoparticles. Such low cytotoxicity indicates that the MSN@C-dots/RB nanoparticles are biocompatible and nearly nontoxic to normal cells.

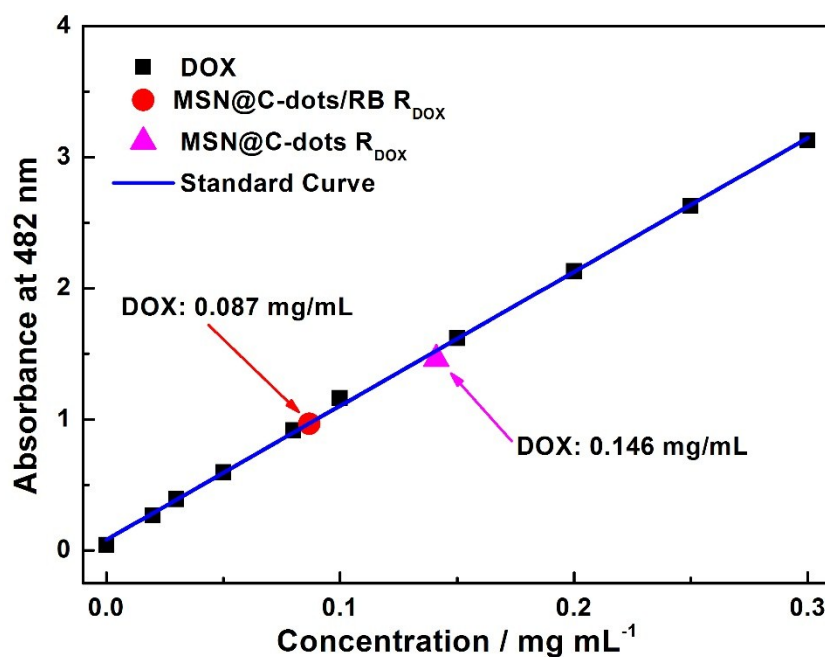


Figure S8. Quantitative analysis of the DOX loading capacity and loading efficiency of the MSN@C-dots/RB nanoparticles. The amount of DOX was determined by measuring the absorbance of DOX at 482 nm. The DOX loading capacity and loading efficiency were calculated as follows: DOX loading capacity (wt %) = (original DOX - DOX in supernatant)/(MSN@C-dots/RB nanoparticles) \times 100 %, and DOX loading efficiency (wt %) = (original DOX - DOX in supernatant)/(original DOX content) \times 100%. From the absorbance data, the DOX content of MSN@C-dots/RB and MSN@C-dots nanoparticles were determined to be 34.4 % and 29.5%, respectively. The DOX loading efficiency were determined to be 82.6% and 70.8%, respectively.

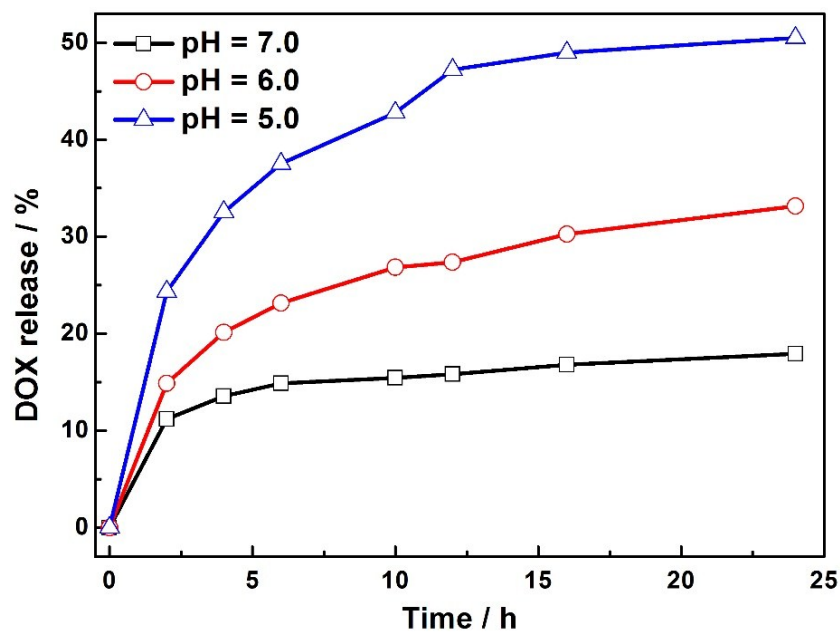


Figure S9. Cumulative DOX release from the MSN@C-dots/RB nanoparticles in PBS buffer at different pH (pH 5.0, 6.0, and 7.0). The release amount of DOX was determined by measuring the absorbance of DOX at 480 nm at determined time points. The cumulative release of DOX was determined as a percentage compared to the loaded DOX within MSN@C-dots/RB nanoparticles.

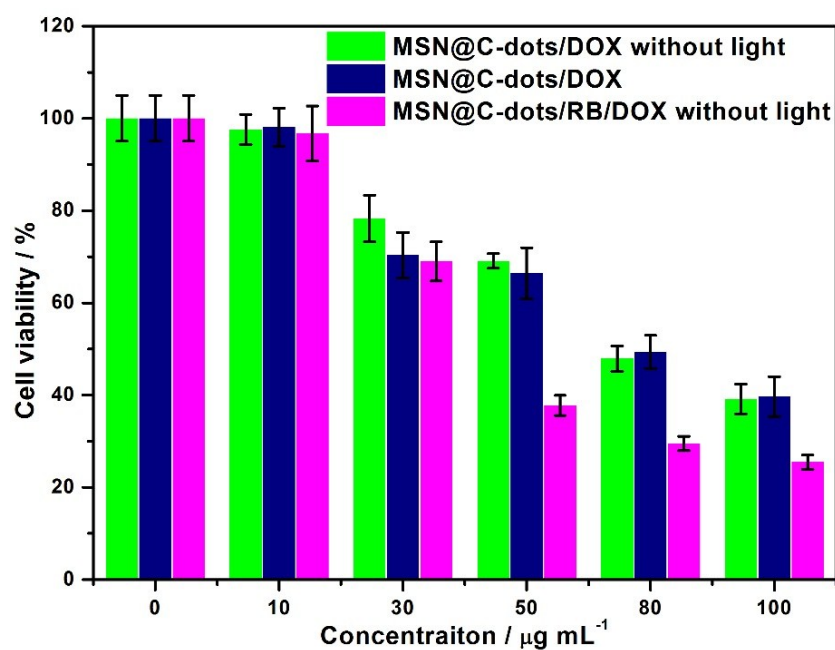


Figure S10. *In vitro* cytotoxicity of MSN@C-dots and MSN@C-dots/RB nanoparticles loaded with DOX against human lung cancer (H1299) cells after incubation for 4 h by using MTT assay. Comparing to the H1299 cells treated with MSN@C-dots/DOX nanoparticles with or without the green light irradiation, a significant reduction in cell viability was observed for cells incubated with MSN@C-dots/RB/DOX without the green light irradiation. This result demonstrated that the MSN@C-dots/RB nanoparticles had higher DOX loading capacity than MSN@C-dots nanoparticles.

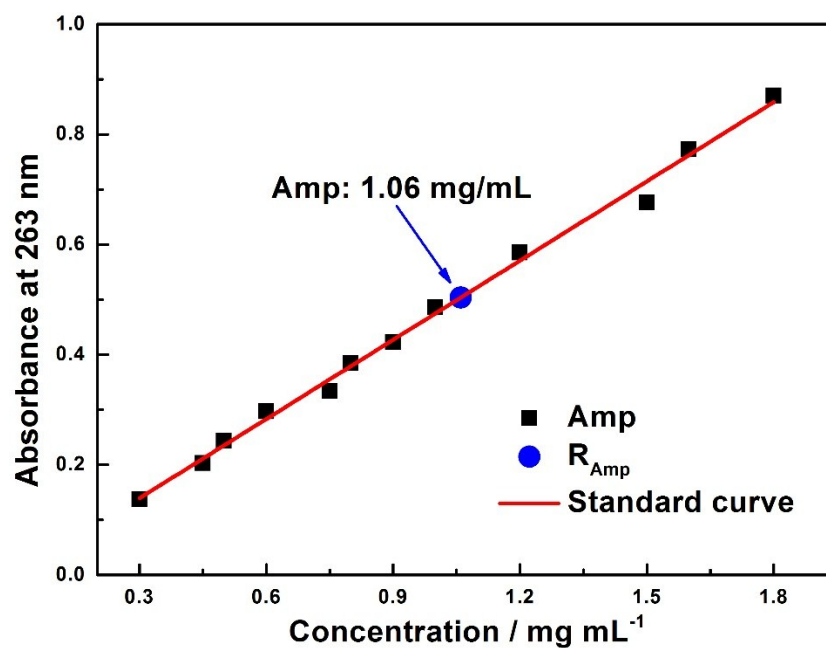


Figure S11. Quantitative analysis of the ampicillin loading capacity and loading efficiency of the MSN@C-dots/RB nanoparticles. The amount of Amp was determined by measuring the absorbance of Amp at 263 nm. The Amp loading capacity and loading efficiency were calculated as follows: Amp loading capacity (wt %) = (original Amp - Amp in supernatant)/(MSN@C-dots/RB nanoparticles) \times 100 %, and Amp loading efficiency (wt %) = (original Amp - Amp in supernatant)/(original Amp) \times 100%. From the absorbance data, the Amp content of MSN@C-dots/RB nanoparticles was quantified to be 18.3% and Amp loading efficiency was quantified to be 29.3%.

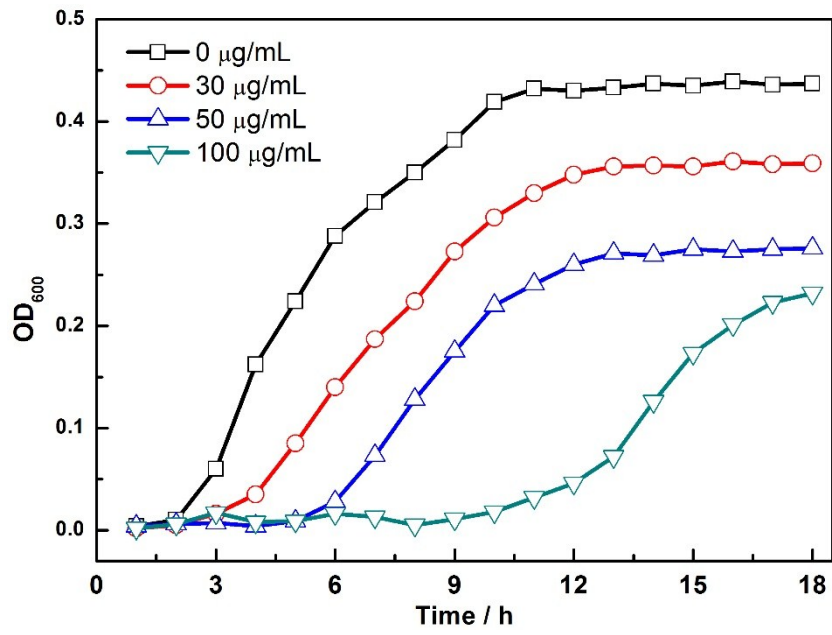


Figure S12. The antibacterial effect of MSN@C-dots/RB/Amp nanoparticles without green light irradiation. The growth of *E. coli* was gradually suppressed with increasing MSN@C-dots/RB/Amp concentration, illustrating the moderate antibacterial effect of Amp.